© 2015. Published by The Company of Biologists Ltd | Journal of Cell Science (2015) 128, 1023–1033 doi:10.1242/jcs.162545

RESEARCH ARTICLE

The focal adhesion protein PINCH-1 associates with EPLIN at integrin adhesion sites

Esra Karaköse[1], Tamar Geiger[2], Kevin Flynn[1], Katrin Lorenz-Baath[1], Roy Zent[3,4], Matthias Mann[2] and Reinhard Fässler[1,*]

ABSTRACT

PINCH-1 is a LIM-only domain protein that forms a ternary complex with integrin-linked kinase (ILK) and parvin (to form the IPP complex) downstream of integrins. Here, we demonstrate that *PINCH-1* (also known as *Lims1*) gene ablation in the epidermis of mice caused epidermal detachment from the basement membrane, epidermal hyperthickening and progressive hair loss. PINCH-1-deficient keratinocytes also displayed profound adhesion, spreading and migration defects *in vitro* that were substantially more severe than those of ILK-deficient keratinocytes indicating that PINCH-1 also exerts functions in an ILK-independent manner. By isolating the PINCH-1 interactome, the LIM-domain-containing and actin-binding protein epithelial protein lost in neoplasm (EPLIN, also known as LIMA1) was identified as a new PINCH-1-associated protein. EPLIN localized, in a PINCH-1-dependent manner, to integrin adhesion sites of keratinocytes *in vivo* and *in vitro* and its depletion severely attenuated keratinocyte spreading and migration on collagen and fibronectin without affecting PINCH-1 levels in focal adhesions. Given that the low PINCH-1 levels in ILK-deficient keratinocytes were sufficient to recruit EPLIN to integrin adhesions, our findings suggest that PINCH-1 regulates integrin-mediated adhesion of keratinocytes through the interactions with ILK as well as EPLIN.

KEY WORDS: Integrin, Focal adhesion, EPLIN, LIMA1, PINCH-1, LIMS1, Keratinocyte, Skin

INTRODUCTION

The skin is composed of an epidermal and a dermal compartment, which are separated by a basement membrane. The primary cell types of the epidermis are keratinocytes, which form different cell layers. The basal cell layer is attached to the basement membrane, displays high proliferative capacity and harbors epidermal stem and progenitor cells. When basal keratinocytes initiate differentiation they exit the cell cycle, detach from the basement membrane and move to the suprabasal layers where they eventually die and slough off as enucleated dead cells (squames).

Adhesion of keratinocytes to the basement membrane and to each other is essential for epidermal development and homeostasis. Keratinocyte adhesion to the underlying basement membrane is mainly mediated by integrins (Watt, 2002). Genetic and cell biological studies have revealed that integrins fine tune multiple functions of basal keratinocytes including basement membrane attachment, proliferation, differentiation, migration and growth factor and cytokine signaling (Dowling et al., 1996; van der Neut et al., 1996; Brakebusch et al., 2000; Raghavan et al., 2000; Grose et al., 2002; Sehgal et al., 2006; Rodius et al., 2007; Margadant et al., 2009; Niculescu et al., 2011). The short integrin cytoplasmic domains lack enzymatic activity for signal transduction, which makes them dependent on the recruitment of adaptor and signaling proteins that assemble into large signaling hubs called focal adhesions (FAs). Integrin-linked kinase (ILK) is an adaptor protein that is recruited to integrin β tails upon integrin–ligand binding. ILK forms a heterotrimeric complex with PINCH and parvin called the IPP complex. The IPP complex is pre-assembled in the cytoplasm and enables FA targeting, stability of its partners, signaling to the actin cytoskeleton and crosstalk with growth factor signaling pathways (Legate et al., 2006; Wickström et al., 2010a; Azimifar et al., 2012). Absence of ILK in basal keratinocytes of skin leads to epidermal adhesion defects and hair loss (Lorenz et al., 2007; Nakrieko et al., 2008). The role of PINCH in skin is not known. There are two PINCH proteins (PINCH-1 and PINCH-2, also known as LIMS1 and LIMS2, respectively); each has five LIM domains followed by a C-terminal nuclear localization signal. The first LIM domain of PINCH-1 and PINCH-2 binds ILK (Zhang et al., 2002; Braun et al., 2003). PINCH-1 is ubiquitously expressed, whereas PINCH-2 is enriched in heart and skeletal muscle and absent in keratinocytes. Deletion of the PINCH-1 gene in mice leads to peri-implantation lethality associated with impaired cell–matrix and cell–cell adhesion (Li et al., 2005; Liang et al., 2005). Deletion of PINCH-2 produces no obvious phenotype (Stanchi et al., 2005). It is believed that PINCH-1 regulates cell adhesion stability and maintenance through ILK, parvin and actin regulatory proteins that associate with the LIM2–LIM5 domains (Tu et al., 1998; Tu et al., 2001; Bock-Marquette et al., 2004; Chiswell et al., 2008; Chiswell et al., 2010).

Keratinocytes develop multiple cell–cell adhesion sites, including adherens junctions, which regulate cell polarity and adhesion between two neighboring cells (Jamora and Fuchs, 2002). Adherens junctions form through homophilic interactions between E-cadherins whose cytoplasmic domains are associated with a filamentous actin belt through a large number of adaptor proteins (Abe and Takeichi, 2008). Recently, epithelial protein lost in neoplasm (EPLIN, also known as LIMA1) has been shown to serve as an adaptor in adherens junctions and to form a ternary complex with α-catenin and F-actin without impairing their binding to β-catenin (Gates and Peifer, 2005; Mège et al., 2006; Abe and Takeichi, 2008; Baum and Georgiou, 2011). EPLIN was

[1]Department of Molecular Medicine, Max Planck Institute of Biochemistry, 82152 Martinsried, Germany. [2]Department of Proteomics and Signal Transductions, Max Planck Institute of Biochemistry, 82152 Martinsried, Germany. [3]Division of Nephrology, Department of Medicine, Vanderbilt Medical Center, Nashville, TN, 37232, USA. [4]Department of Medicine, Nashville Veterans Affairs Medical Center, Nashville, TN, 37232, USA.

*Author for correspondence (faessler@biochem.mpg.de)

Received 1 September 2014; Accepted 2 January 2015

Journal of Cell Science (2015) 128, 1023–1033 doi:10.1242/jcs.162545

originally identified in a screen designed to identify proteins that are significantly downregulated or lost in human cancer cells (Maul and Chang, 1999). The EPLIN protein consists of two actin-binding domains (ABDs) separated by a central LIM domain. Two alternatively spliced EPLIN mRNAs have been described, which are translated into a 90 kDa and 110 kDa protein. The function of EPLIN is poorly understood. It has been shown that the two ABDs bundle filamentous actin (Maul et al., 2003; Schaller et al., 2013) and that ERK1/2 is able to phosphorylate EPLIN, which inhibits F-actin binding resulting in the translocation of EPLIN to the cell periphery and dorsal membrane ruffles (Han et al., 2007). Moreover, EPLIN has recently been shown to localize to FAs, where it interacts with paxillin and possibly stabilizes FAs (Tsurumi et al., 2014).

To directly analyze PINCH-1-regulated cell adhesion in epidermis and hair follicles, we deleted the *PINCH-1* gene in basal keratinocytes using the Cre/loxP system. The mutant mice suffer from epidermal blisters and hyperthickening, progressive hair loss and cell–matrix adhesion defects. PINCH-1-deficient keratinocytes display severe adhesion, spreading and migration defects. Immunoprecipitation of PINCH-1 from keratinocyte lysates combined with mass spectrometry identified EPLIN as a new PINCH-1 interaction partner. Cell biological studies with primary keratinocytes revealed that EPLIN recruitment to cell–matrix adhesion sites is controlled by PINCH-1, whereas PINCH-1 recruitment to FAs is not grossly affected in EPLIN-depleted cells. The implications of our findings are discussed.

RESULTS

PINCH-1 is important for skin homeostasis

To directly study the function of PINCH-1 in the epidermis we crossed mice carrying a *loxP*-flanked *PINCH-1* gene (PINCH-1$^{fl/fl}$) (Li et al., 2005) with mice expressing the *Cre* recombinase under control of the keratin 5 (K5, also known as KRT5) promoter (K5-Cre) (Ramirez et al., 2004). The number of mice with the floxed *PINCH-1* gene and the K5-Cre transgene was low (one out of 45 offspring) suggesting that the two genes reside in close proximity on the same chromosome. PINCH-1$^{fl/wt}$ mice with and without the K5-Cre transgene were normal and served as controls (control). Mice with two floxed PINCH-1 alleles and the K5-Cre transgene (P1-K5) were viable (Fig. 1A). Western blotting (WB) of epidermal lysates and immunostaining of back skin from P1-K5 mice with antibodies that recognizes either PINCH-1 or both PINCH-1 and PINCH-2 revealed an almost complete loss of PINCH protein, which was accompanied by diminished ILK levels (supplementary material Fig. S1A–D). Although P1-K5 mice were normal at birth, their hair appeared shaggy with small areas of alopecia appearing at postnatal day 14 (P14) (Fig. 1A). By P56 P1-K5 mice had lost their hair and developed a patchy pigmentation of their skin (Fig. 1A). Given that PINCH-2 was not expressed *de novo* in P1-K5 keratinocytes (supplementary material Fig. S1B,C), the low levels of PINCH-1 protein in P56 epidermal lysates indicates that cells escaping K5-Cre-mediated PINCH-1 gene deletion expanded in the epidermis of P1-K5 mice. To avoid the presence of PINCH-1-expressing cells in our analyses, all skin histology and cell biology studies with primary keratinocytes were conducted with P1-K5 mice that were 2 weeks of age or younger.

Hematoxylin-eosin (H&E) staining of the back skin revealed that the P14 skin of P1-K5 mice contained sparse and abnormal hair follicles, a hyperthickened interfollicular epidermis (IFE) and small blisters at the dermal–epidermal junctions (DEJ)

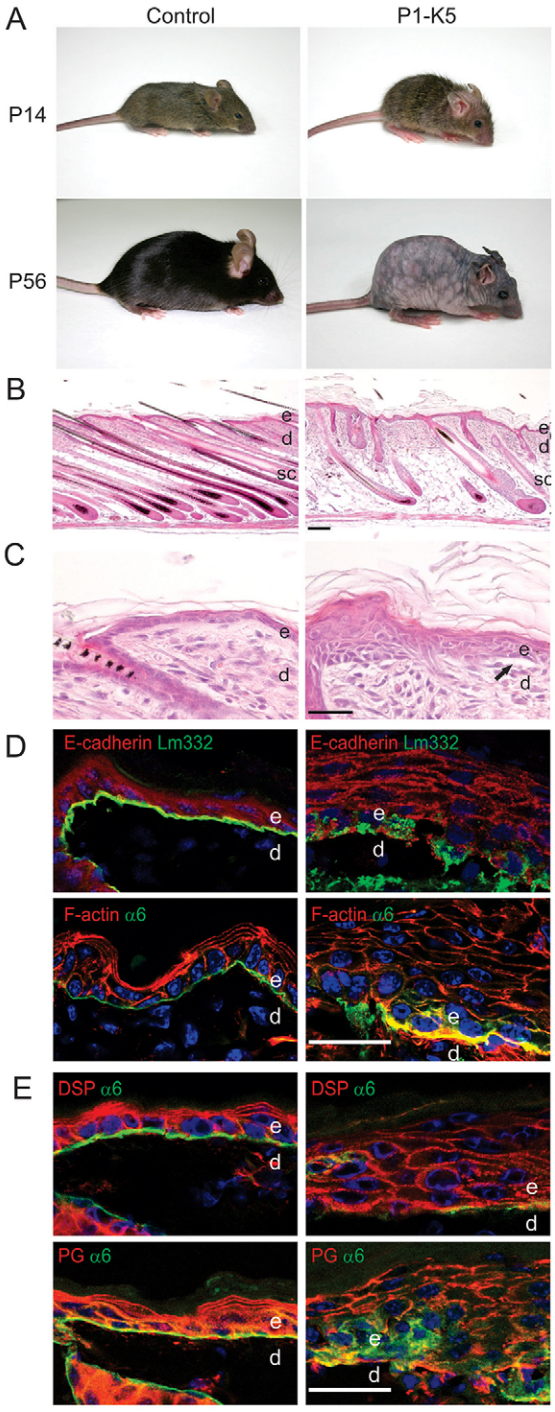

Fig. 1. K5-Cre-mediated deletion of PINCH-1. (A) Control and P1-K5 animals at 2 and 8 weeks of age. (B) H&E staining of back skin sections from 2-week-old mice. (C) Close-up view of H&E staining of back skin sections from 2-week-old mice. The arrow in the right panel indicates a blister. (D,E) Immunofluorescence of back skin from P14 control and P1-K5 mice for E-cadherin, Lm332, F-actin, desmoplakin (DSP), plakoglobin (PG) and α6 integrin. e, epidermis; d, dermis; sc, subcutis. Scale bars: 100 μm (B,C); 50 μm (D,E).

(Fig. 1B,C). When quantified, the numbers of blisters per millimeter skin were significantly ($P<0.001$) higher in P1-K5 skin (supplementary material Fig. S1E). The proliferating cells determined by Ki67 staining were 50% of the total basal cell

Journal of Cell Science (2015) 128, 1023–1033 doi:10.1242/jcs.162545

number both in control and P1-K5 epidermis. Interestingly, 20% of the total cell number in the suprabasal layers of P1-K5 epidermis was also Ki67+, which was observed in less than 5% of the suprabasal cells in the control skin (supplementary material Fig. S1F), pointing to an adhesion defect and loss of proliferating P1-K5 basal keratinocytes. Hair follicle morphogenesis in control mice was complete at P14 and all hair follicles resided deep in the subcutis (Fig. 1B, left panel). In contrast, P1-K5 skin exhibited two types of hair follicles; fully developed hair follicles with hyperthickened outer root sheaths (ORS) reaching the subcutis, and short hair follicles with an abnormal shape residing in the dermis and with either a distorted or no dermal papilla attached to them (Fig. 1B, right panel; supplementary material Fig. S1G, right panel).

The deposits of laminin 332 (Lm322) and nidogen, two major components of the epidermal–dermal basement membrane, and the expression of α6 integrin appeared as continuous layers between epidermis and dermis of control skin. In P1-K5 skin the Lm322 and nidogen deposits and α6 integrin localization were also frequently detected on the apical and lateral sides of basal keratinocytes (Fig. 1D,E; supplementary material Fig. S1H). F-actin, the cell–cell adhesion protein E-cadherin, as well as desmosomal plaque proteins desmoplakin and plakoglobin localized to the subcortical lateral and apical regions of basal keratinocytes in control skin. In basal P1-K5 keratinocytes, however, E-cadherin and F-actin extended to the basal sides suggesting that cell polarity is distorted (Fig. 1D,E). These findings demonstrate that PINCH-1 plays a role in cell–matrix adhesion stability, basement membrane integrity and keratinocyte polarity.

PINCH-1 controls matrix adhesion, spreading and migration of keratinocytes

PINCH and ILK are obligate binding partners (Legate et al., 2006), and loss of ILK severely compromises integrin-mediated functions of keratinocytes (Lorenz et al., 2007). To compare cell–matrix adhesion and spreading between P1-K5 and ILK-deficient keratinocytes (ILK-K5), we derived primary keratinocytes from both mouse strains and performed plate and wash assays by seeding them on laminin-322 (Lm322), fibronectin or collagen I (Col1). As expected, control keratinocytes readily adhered to the three matrix substrates, whereas adhesion of P1-K5 as well as ILK-K5 keratinocytes to Lm332, fibronectin and Col1 was significantly ($P<0.001$) impaired (Fig. 2A). The P1-K5 and ILK-K5 keratinocytes that were able to adhere showed severely impaired spreading, even 20 h after seeding on a mixture of fibronectin and Col1 matrix (Fig. 2B–D). Interestingly, the spreading defect of P1-K5 cells was more pronounced when compared to ILK-K5 cells (Fig. 2B). Immunostaining of control cells revealed numerous FAs containing ILK and PINCH that were linked to F-actin stress fibers (Fig. 2C,D). ILK-K5 cells developed paxillin-positive FAs linked to thin actin fibers and thick subcortical actin deposits (Fig. 2C). P1-K5 cells also formed small, paxillin-positive adhesion sites and accumulated a thick layer of F-actin beneath the cell cortex (Fig. 2D). Given that cell adhesion and spreading are important parameters of cell migration, we analyzed migration of P1-K5 keratinocytes by performing scratch wound assays and found that control keratinocytes closed the wound within 12–24 h, whereas P1-K5 cells were unable to move into the wounded area (Fig. 2E). To exclude that the decreased P1-K5 keratinocyte migration, spreading and adhesion result from altered integrin expression and/or activation, we isolated primary keratinocytes, determined integrin levels and the level of the 9EG7 epitope, which binds the active conformation of β1 integrin (Lenter et al., 1993). The experiments revealed that the levels of all integrins tested as well as the levels for the 9EG7 epitope were similar between control and P1-K5 cells (supplementary material Fig. S2A). Taken together, these results demonstrate a strong role for PINCH-1 in cell adhesion, spreading and migration.

Although E-cadherin and F-actin distribution were altered in basal keratinocytes *in vivo*, cell–cell adhesion formation induced with Ca^{2+} occurred in primary (P1-K5) as well as immortalized PINCH-$1^{-/-}$ keratinocytes when they were plated on a mixed fibronectin and Col1 matrix (Fig. 2F). The F-actin distribution resembled the *in vivo* situation with large deposits at the basal side (Fig. 2F; supplementary material Fig. S2B) and the *z*-axis views revealed an increased cell thickness, irregular cell shapes and stacking (Fig. 2F, lower strips). These findings and the absence of skin barrier defects (data not shown) indicate that loss of PINCH-1 expression in keratinocytes enables the formation of cell–cell adhesion sites but severely impairs the formation and functions of cell–matrix adhesion sites.

PINCH-1 interacts with EPLIN at integrin adhesion sites

To dissect mechanistically how PINCH-1 supports keratinocyte adhesion, spreading and migration, we screened for new interaction partners by performing label-free pulldown experiments with immortalized PINCH-$1^{-/-}$ keratinocytes rescued with an EGFP-tagged PINCH-1 (PINCH1^{rescued}) followed by mass-spectrometry (supplementary material Fig. S2C). The PINCH-$1^{-/-}$ cells were derived from immortalized PINCH-1 fl/fl keratinocytes and subjected to adenoviral Cre transduction. They phenocopied the severe defects of primary P1-K5 cells, and reconstitution with EGFP-tagged PINCH-1 restored adhesion, spreading, F-actin distribution and expression of ILK and parvin (supplementary material Fig. S2D–F).

Among the proteins that were precipitated with PINCH-1 we identified known PINCH-1 interactors such as ILK and Rsu1 as well as new binding partners such as EPLIN (Fig. 3A; supplementary material Table S1). Given that EPLIN was among the top hits in our interactome screen and has also been identified as a mechanosensitive component of focal adhesions in recent proteomic screens (Schiller et al., 2011; Schiller et al., 2013), we further characterized the role of the PINCH-1–EPLIN interaction. Consistent with the proteomics data, endogenous EPLIN was co-immunoprecipitated with GFP–PINCH-1 (Fig. 3B), and endogenous PINCH-1 co-immunoprecipitated with EPLIN–GFP (Fig. 3C). Importantly, immunoprecipitation of endogenous PINCH-1 also co-precipitated endogenous EPLIN (Fig. 3D), clearly demonstrating that the two endogenous proteins associate in keratinocytes. Interestingly, α-catenin, a well-known EPLIN-binding partner (Abe and Takeichi, 2008), co-precipitated with EPLIN–GFP expressed in control or PINCH-$1^{-/-}$ keratinocytes indicating that EPLIN binding to α-catenin is independent of PINCH-1. Finally, we performed proximity ligation assays (PLAs) in PINCH-$1^{fl/fl}$ and PINCH1^{rescued} keratinocytes. We observed no PLA signal when the assay was performed with no antibody or only with anti-EPLIN or anti-PINCH-1 antibodies (supplementary material Fig. S3A). However, when cells were incubated with both anti-EPLIN and anti-PINCH-1 antibodies the PLA signal was strong and colocalized with paxillin (Fig. 3E; supplementary material Fig. S3A) indicating that EPLIN and PINCH-1 reside in close proximity in FAs.

Journal of Cell Science (2015) 128, 1023–1033 doi:10.1242/jcs.162545

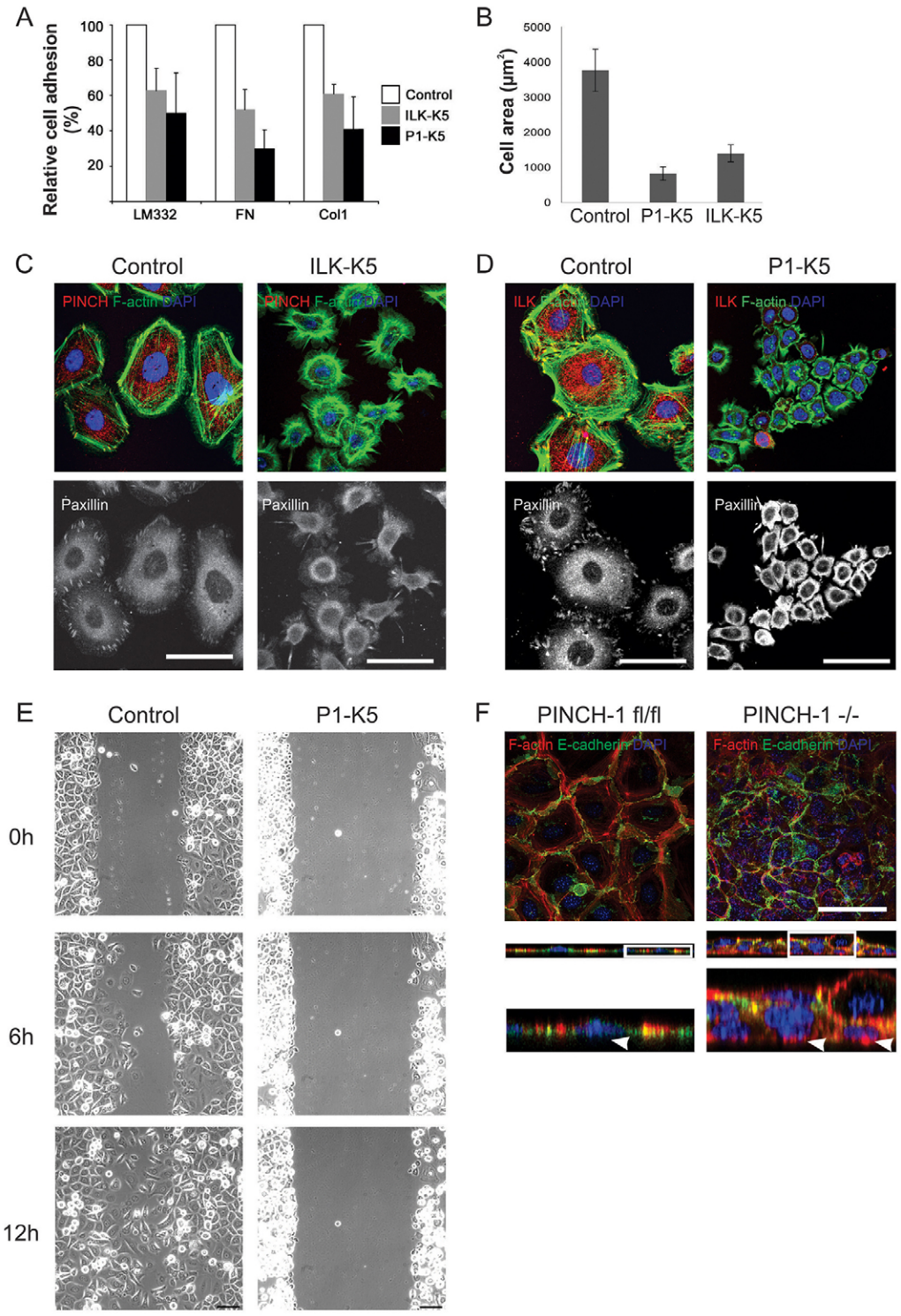

Fig. 2. P1-K5 keratinocytes display severe spreading and adhesion defects. (A) Quantification of adhesion on LM332, fibronectin (FN) and Col1. Results are represented relative to control cells. Results are the mean±s.d. of three independent experiments. (B) Quantification of spreading area of 100 primary keratinocytes from each genotype. Results are the mean±s.d. of three independent experiments. (C) Immunostaining of primary control and ILK-K5 keratinocytes for PINCH-1, F-actin and paxillin. (D) Immunostaining of primary control and P1-K5 keratinocytes for ILK, F-actin and paxillin. (E) Time lapse microscopy of a cell wound scratch assay. (F) 3D reconstruction of confocal stacks of keratinocytes grown on a fibronectin and Col1 matrix after differentiation with $CaCl_2$, stained for F-actin and E-cadherin. The strips at the bottom of the images indicate a cross-section of a 3D confocal projection; the area indicated by the box is magnified in the lower image. Arrowheads depict an abnormal F-actin distribution at the bottom side of the PINCH-1$^{-/-}$ cells. Scale bars: 50 µm (C,D,F); 100 µm (E).

PINCH-1 regulates EPLIN localization to cell–matrix adhesions

In agreement with previous reports (Abe and Takeichi, 2008), we also found EPLIN together with E-cadherin at cell–cell adhesion sites of densely seeded and Ca^{2+}-treated control keratinocytes (Fig. 4A). In Ca^{2+}-treated P1-K5 cells EPLIN was found at cell–cell adhesion sites and dispersed through the cytoplasm *in vitro* (Fig. 4A) and *in vivo* (Fig. 4B; supplementary material Fig. S3B). When untreated control keratinocytes were sparsely seeded on a fibronectin and Col1 matrix we observed a strong colocalization of EPLIN with paxillin in FAs (Fig. 4C). In contrast, EPLIN was absent from FAs of sparsely seeded PINCH-1$^{-/-}$ keratinocytes and instead accumulated in the cytoplasm (Fig. 4C). Similarly, skin sections of P1-K5 mice showed regions of poor EPLIN localization at the basal side of basal keratinocytes and abnormal accumulations in the cytoplasm, whereas EPLIN at sites of cell–cell interaction was not grossly altered (Fig. 4B; supplementary material Fig. S3B). Interestingly, western blotting revealed

Journal of Cell Science (2015) 128, 1023–1033 doi:10.1242/jcs.162545

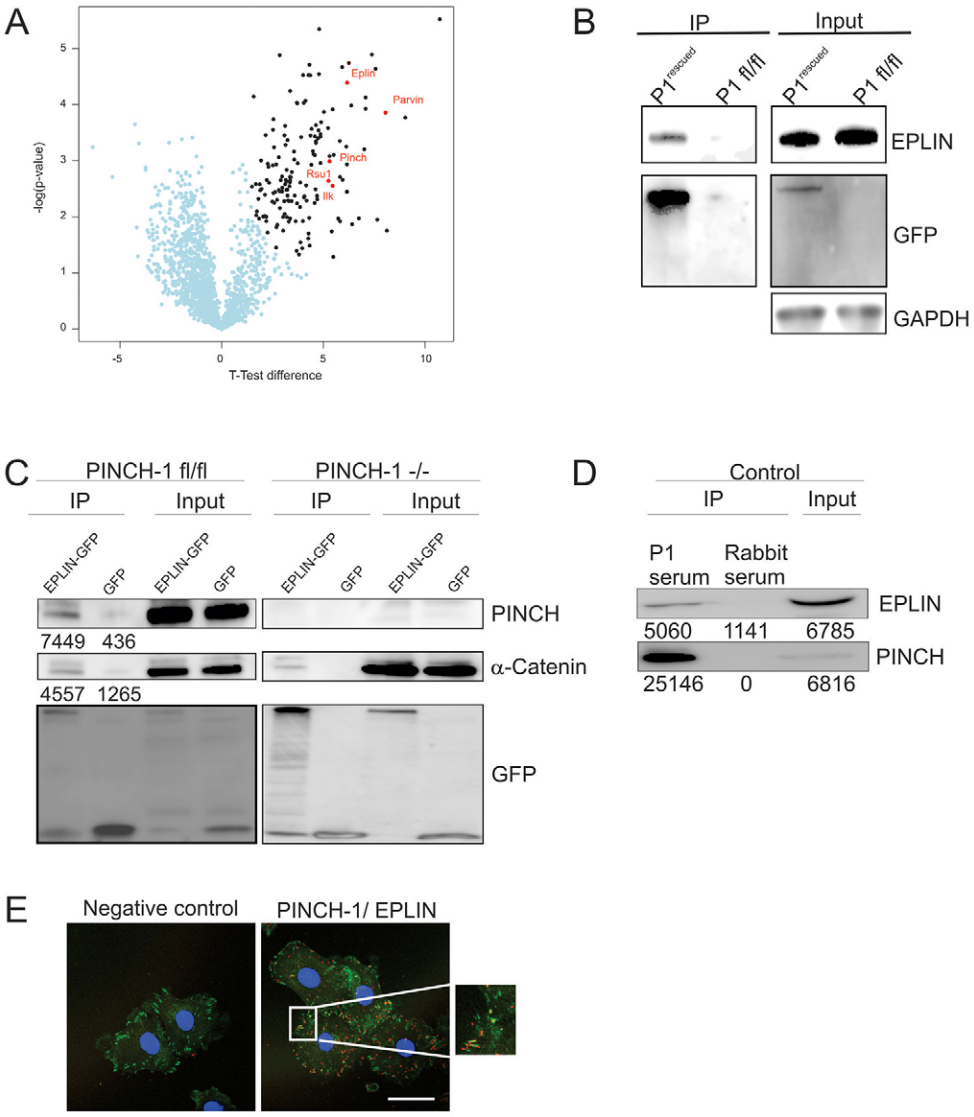

Fig. 3. EPLIN is a new PINCH-1-interacting protein. (A) Volcano plot of GFP immunoprecipitates identified by label-free mass spectrometry performed with PINCH-1$^{fl/fl}$ (P1 fl/fl) and PINCH-1$^{-/-}$ cells rescued with EGFP-tagged PINCH-1 (P1^{rescued}) following GFP immunoprecipitation (IP). (B) GFP immunoprecipitation of PINCH-1$^{fl/fl}$ and rescued PINCH-1cells immunoblotted with an antibody against EPLIN. Note that EPLIN can only be co-immunoprecipitated when GFP-tagged PINCH-1 is present. Whole-cell lysates are shown as the input. (C) GFP immunoprecipitation of EGFP-tagged EPLIN-expressing PINCH-1$^{fl/fl}$ and PINCH-1$^{-/-}$ cells immunoblotted with antibodies against PINCH and α-catenin. Cells were transfected either with EPLIN–GFP or GFP. Whole-cell lysates are shown as the input. Numbers beneath blots indicate the mean signal intensity of the respective band in three independent experiments. (D) PINCH-1 immunoprecipitates from PINCH-1$^{fl/fl}$ cells immunoblotted with polyclonal rabbit anti-EPLIN and anti-PINCH-1 antiserum. Normal rabbit serum was used as negative control. Whole-cell lysates are shown as the input. Numbers beneath the blots indicate the mean signal intensity of the respective band from three independent experiments. (E) A PLA on PINCH-1$^{fl/fl}$ cells was performed and immunostained for paxillin. Red signal indicates that PINCH-1 and EPLIN are in close proximity. The magnified image shows red signal overlapping with paxillin (green) in FAs. Scale bar: 50 μm.

slightly reduced EPLIN protein levels in P1-K5 keratinocytes (Fig. 4D) suggesting that the PINCH-1–EPLIN interaction stabilizes the EPLIN protein. To determine whether the reduced EPLIN levels caused the reduced EPLIN staining in FAs and the impaired spreading, we increased EPLIN levels by overexpressing EGFP-tagged EPLIN in PINCH-1$^{-/-}$ keratinocytes and found that overexpressed EPLIN neither localized to cell–matrix adhesions nor rescued the spreading defect (Fig. 4E).

Next, we investigated whether PINCH-1 recruitment to integrin adhesion sites was dependent on EPLIN. To this end, we efficiently depleted EPLIN in control cells using specific small interfering RNAs (siRNAs) and found that ILK and PINCH-1 levels became slightly reduced (Fig. 5A) and E-cadherin levels decreased at AJs (supplementary material Fig. S3C). Despite the presence of substantial levels of PINCH-1 and ILK in FAs of EPLIN-depleted cells, their spreading and migration in wound closure assays were impaired (Fig. 5B–D). Taken together, these findings indicate that EPLIN is a new PINCH-1 interacting protein that is recruited to FAs in a PINCH-1-dependent manner and regulates adhesion, spreading and migration.

ILK is not required to localize EPLIN to cell–matrix adhesion sites

To investigate whether the recruitment of EPLIN to FAs requires an intact IPP complex, we isolated primary ILK-K5 keratinocytes and immunostained them for EPLIN (Lorenz et al., 2007). The poorly spreading ILK-K5 keratinocytes contained large FAs that were positive for EPLIN (Fig. 6A) suggesting that the remaining PINCH-1 protein in ILK-deficient cells is sufficient to support EPLIN recruitment to FAs independently of an intact IPP complex (Lorenz et al., 2007). Although western blotting showed low levels of PINCH in ILK-K5 cells (Fig. 6B), immunostaining failed to detect these low PINCH-1 levels in FAs owing either to the decreased protein levels and/or to the quality of the anti-PINCH antibodies (Fig. 6C). To circumvent immunostaining with antibodies, we expressed GFP-tagged PINCH-1 and Cherry-tagged paxillin cDNAs in control and ILK-K5 cells and performed total internal reflection fluorescence (TIRF) microscopy to visualize EGFP–PINCH-1 in FAs. The experiments revealed that GFP-tagged PINCH-1 indeed colocalized with paxillin in FAs of ILK-K5 keratinocytes seeded on a fibronectin and Col1 matrix (Fig. 6D). Taken

Journal of Cell Science (2015) 128, 1023–1033 doi:10.1242/jcs.162545

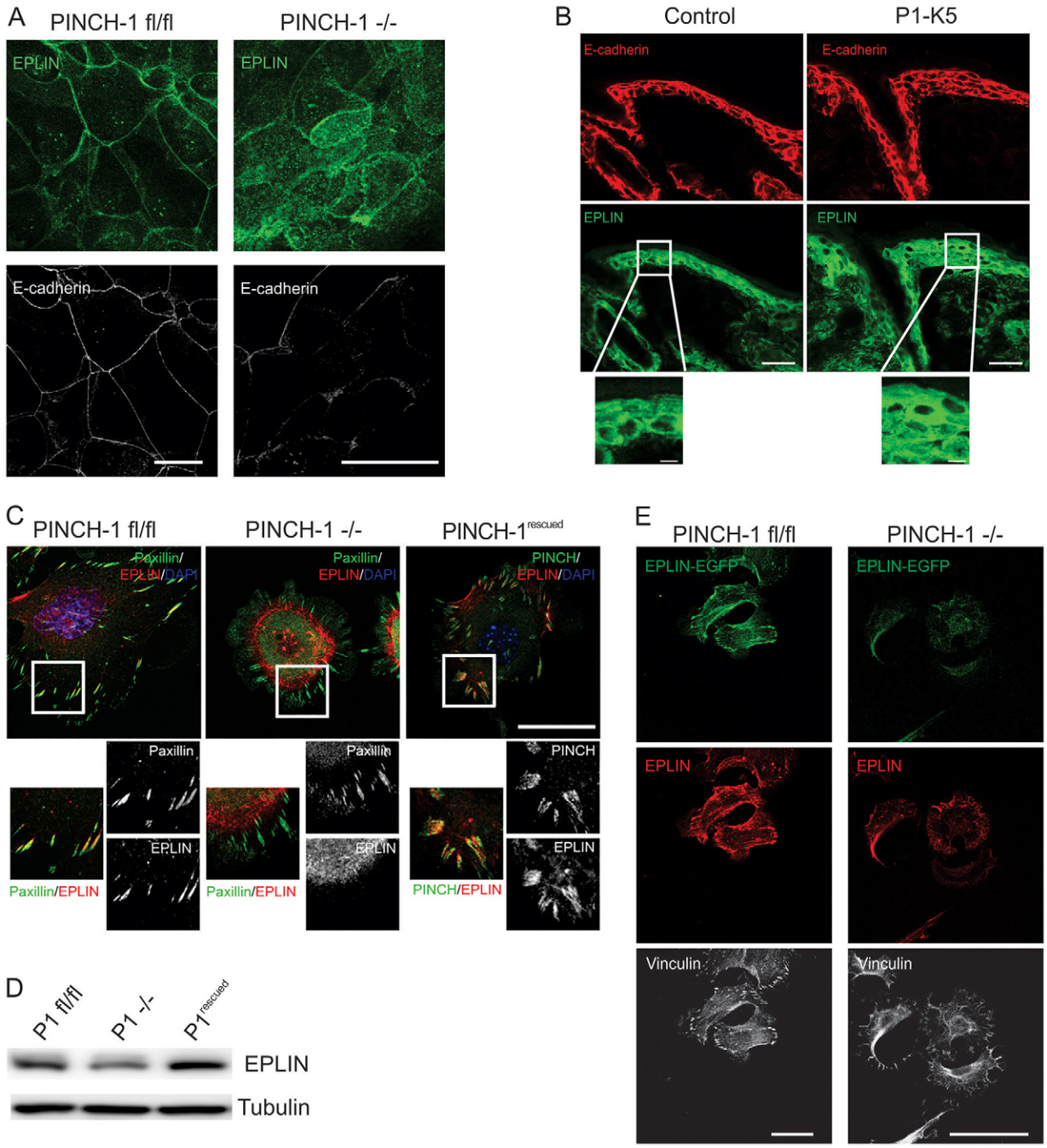

Fig. 4. PINCH-1 regulates EPLIN recruitment to FAs. (A) Immunostaining for EPLIN and E-cadherin of $CaCl_2$-treated keratinocytes. (B) Immunostaining of P14 back skin sections from control and P1-K5 mice for EPLIN and E-cadherin. (C) Immunostaining for EPLIN, paxillin, and PINCH of PINCH-$1^{fl/fl}$, PINCH-$1^{-/-}$ and PINCH-$1^{rescued}$ cells. In PINCH-$1^{-/-}$ keratinocytes EPLIN fails to colocalize with paxillin in FAs. The area indicated by the box is shown as a magnified image below each figure. (D) Western blot analysis of EPLIN in PINCH-1 (P1) fl/fl, PINCH-$1^{-/-}$ and PINCH$1^{rescued}$ cells. (E) Overexpression of EGFP-tagged EPLIN in PINCH-$1^{fl/fl}$ and PINCH-$1^{-/-}$ cells immunostained for EPLIN and Vinculin. Scale bars: 50 µm.

together, these data indicate that PINCH-1 can localize to ILK-deficient FAs and that the low PINCH-1 levels in ILK-K5 keratinocytes are sufficient to recruit EPLIN to these sites.

DISCUSSION

In this study, we deleted the *PINCH-1* gene in keratinocytes of mice and showed that loss of PINCH-1 expression leads to blisters at the sub-epidermal basement membrane, epidermal hyperplasia and impaired downward growth of hair follicles. Similar defects develop when the β1 integrin or ILK genes are deleted in keratinocytes of mice, and thus this finding supports the common view that ILK and PINCH-1 are essential adaptors downstream of integrins. A careful comparison of keratinocytes from mice lacking either ILK or PINCH-1 revealed that loss of PINCH-1 induces more severe adhesion, spreading and migration defects than loss of ILK.

PINCH-1 is believed to perform its functions in association with ILK and parvin. Contrary to the view that members of the

Journal of Cell Science (2015) 128, 1023–1033 doi:10.1242/jcs.162545

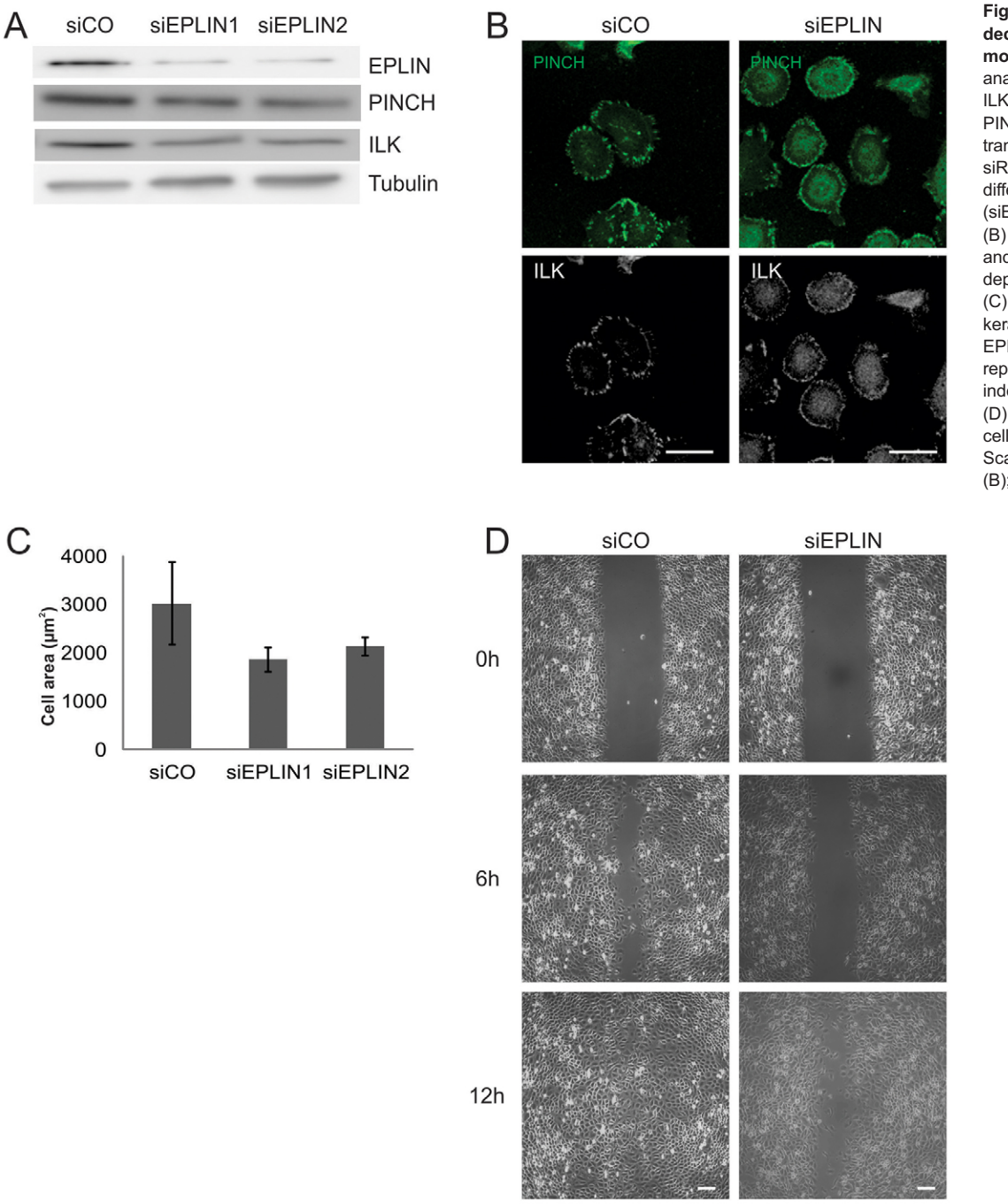

Fig. 5. EPLIN knockdown decreases cell spreading and motility. (A) Western blot analysis of EPLIN, PINCH and ILK in protein lysates from PINCH-1$^{fl/fl}$ keratinocytes transfected with either control siRNA (siCO) or one of two different siRNAs against EPLIN (siEPLIN1 and siEPLIN2). (B) Immunostaining of PINCH and ILK in control or EPLIN-depleted cells. (C) Quantification of keratinocyte spreading after EPLIN depletion. Results represent mean±s.d. of three independent experiments. (D) Time lapse microscopy of cell wound scratch assays. Scale bars: 50 μm (B); 100 μm (D).

IPP complex require each other for stability, deletion of either IPP component does not result in a complete destabilization of the remaining binding partners, as their low levels can be detected by western blotting or mass spectrometry (Lorenz et al., 2007; Fielding et al., 2008a; Fielding et al., 2008b). It is likely that IPP proteins not incorporated into the IPP complex have IPP-independent functions, either within or outside integrin adhesion sites. Indeed, ILK for example, has been shown to localize to centrosomes without PINCH or parvin where it controls spindle organization in mitosis (Fielding et al., 2008a; Fielding et al., 2008b). There is no report of PINCH-1 so far, that demonstrates a subcellular localization of a PINCH-1 fraction that is not destabilized upon loss of ILK deletion. However, it is clear from our study that low levels of PINCH-1 remain in ILK-deficient keratinocytes, although they are difficult to visualize with the available antibodies. To better visualize these low PINCH-1 levels, we tagged PINCH-1 with EGFP, expressed the fusion protein in ILK-deficient cells and observed it in integrin adhesion sites using TIRF microscopy. Although the majority of the PINCH-1 pool was recruited to FAs in an ILK-dependent manner, a small pool of PINCH-1 could be found in FAs in the absence of ILK. The ILK-independent role of PINCH-1 at FAs might explain why the spreading and adhesion defects of PINCH-1-null cells are more severe than those of ILK-null keratinocytes. How the ILK-independent pool of PINCH-1 is recruited to FAs is not clear.

How is the ILK-independent PINCH-1 operating at FAs? To address this question, we performed pulldown experiments

Journal of Cell Science (2015) 128, 1023–1033 doi:10.1242/jcs.162545

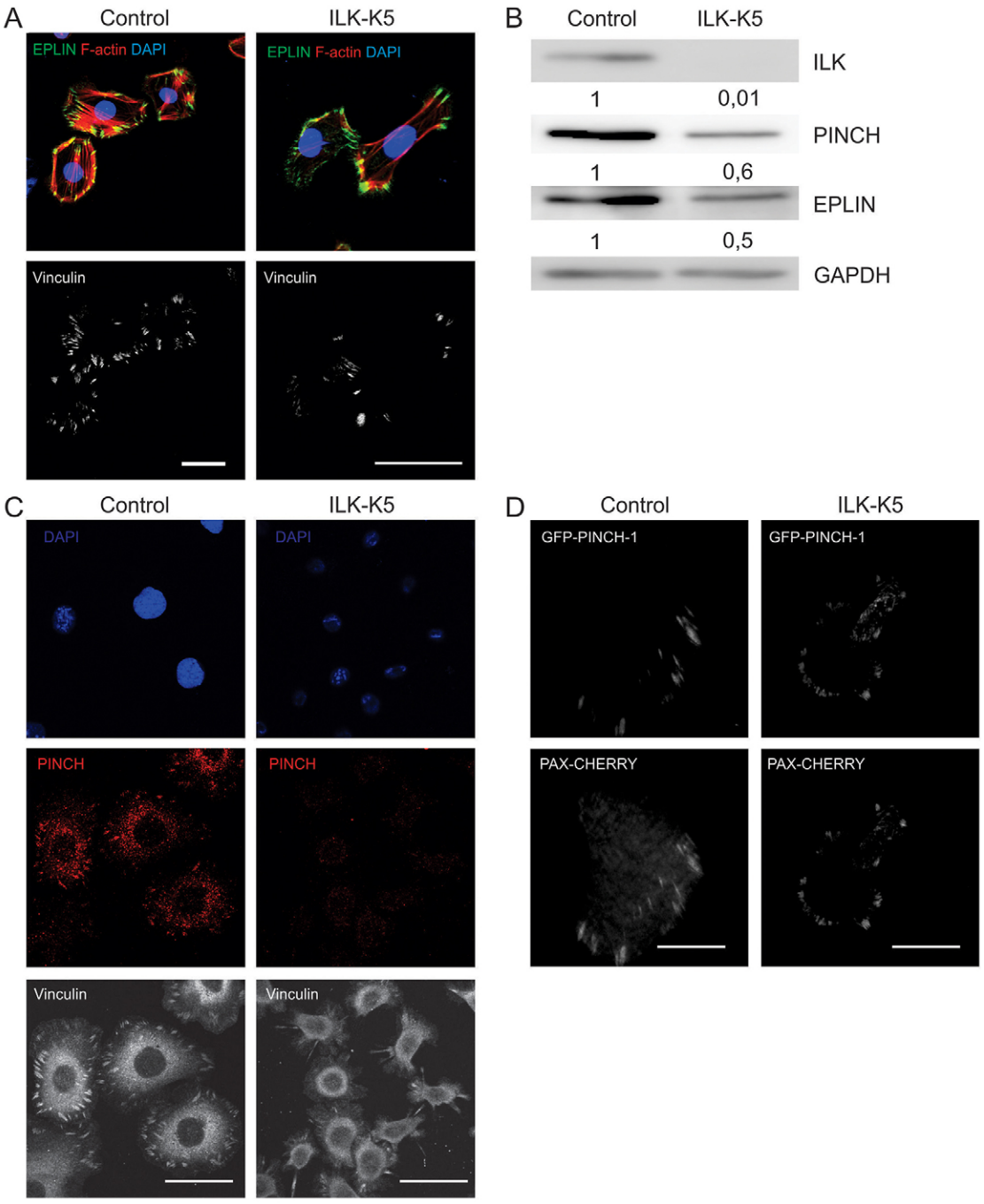

Fig. 6. Recruitment of EPLIN to FAs by PINCH can occur independently of ILK. (A) Immunostaining for EPLIN, vinculin and F-actin in primary control and ILK-K5 cells. Note that the absence of ILK allows FA localization of EPLIN. (B) Western blot analysis of ILK, PINCH and EPLIN in primary control and ILK-K5 cells. GAPDH served as loading control. Numbers beneath the blots indicate relative expression of each protein normalized to GAPDH. (C) Immunostaining for PINCH and vinculin in primary control and ILK-K5 keratinocytes. (D) TIRF image of control and ILK-K5 cells overexpressing GFP–PINCH-1 and Paxillin–Cherry.

followed by mass spectrometry and identified EPLIN as a new PINCH-1-interacting protein. EPLIN is known to bind to α-catenin in cell–cell junctions (Abe and Takeichi, 2008) and is present in the adhesome of fibroblasts (Schiller et al., 2011; Schiller et al., 2013) and FAs of mesangial cells (Tsurumi et al., 2014). Whether the interaction between PINCH-1 and EPLIN is direct or indirect is not clear, as our attempts to purify recombinant PINCH-1 for *in vitro* binding assays were unsuccessful. However, we made several observations pointing to a functional interdependence of PINCH-1 and EPLIN in FAs. First, proximity ligation assays revealed that PINCH-1 and EPLIN reside in close proximity in FAs. Second, PINCH-1 promotes EPLIN stability and induces the recruitment of EPLIN to FAs. Western blotting and immunostaining demonstrated that the levels of EPLIN in whole-cell lysates and the levels of EPLIN in FAs were diminished in PINCH-1-deficient keratinocytes. Although re-expression of PINCH-1 restored total EPLIN levels and EPLIN recruitment to FAs in PINCH-1-deficient keratinocytes,

overexpression of EPLIN in PINCH-1-deficient cells was not sufficient to target EPLIN to FAs, indicating that EPLIN stability and FA recruitment depends on PINCH-1. Third, loss of PINCH-1 or depletion of EPLIN in keratinocytes share similar integrin-dependent defects including impaired cell adhesion, spreading and migration. Finally, our proteomics study revealed a further interesting commonality with respect to the mechanosensitivity of EPLIN and PINCH-1 (Schiller et al., 2011; Schiller et al., 2013); both are among the LIM-domain-containing proteins that require myosin-II-mediated force for their recruitment to and maintenance in FAs (Schiller et al., 2011). Interestingly, a previous paper also reported a force-dependent localization of EPLIN to cell–cell adhesion sites (Taguchi et al., 2011), where EPLIN links the E-cadherin–catenin complex to F-actin (Maul and Chang, 1999; Maul et al., 2003; Abe and Takeichi, 2008).

Given that neither loss of PINCH-1 nor depletion of EPLIN impairs the surface expression or activation state of β1 integrins, we propose that the defects caused by loss of PINCH-1 or EPLIN are due to abnormal adhesion signaling and actin dynamics. PINCH-1 might regulate adhesions and actin dynamics through ILK and/or Nck-2, which can interact with p21-activated kinase (Bokoch et al., 1996), Wiskott–Aldrich syndrome protein (Braverman and Quilliam, 1999) and DOCK180 (Tu et al., 2001), respectively. EPLIN might execute its functions through interaction partners in FAs as well as the ability to crosslink actin filaments into bundles and to fine tune Arp2/3-mediated branching of actin (Han et al., 2007; Schaller et al., 2013). EPLIN interaction partners in FAs are PINCH-1 (shown in this paper) and paxillin (Tsurumi et al., 2014). Interestingly, Tsurumi et al. (Tsurumi et al., 2014) showed that depletion of EPLIN in mesangial cells enhanced rather than reduced their migration. This is in stark contrast to our findings, which revealed a pronounced migration defect upon EPLIN depletion. An explanation for this discrepancy could be that FA signaling and/or actin remodeling are differently controlled by EPLIN and paxillin in different cell types. Keratinocytes are highly motile both in cell culture and during wound closure, whereas mesangial cells are stationary, smooth-muscle-like cells regulating intra-glomerular capillary flow and glomerular ultrafiltration (Schlöndorff and Banas, 2009). Clearly, genetic studies of EPLIN in mice and cells will cast light on its role in different cell types during development and postnatal homeostasis.

MATERIALS AND METHODS

Mouse strains and cells

To obtain a keratinocyte-restricted deletion of the PINCH-1 gene, PINCH-1$^{fl/wt}$ males expressing *Cre* under the control of the keratin 5 promoter were crossed with PINCH-1$^{fl/fl}$ females (Li et al., 2005). Offspring were genotyped as described previously (Li et al., 2005). Primary keratinoyctes were isolated and cultured from PINCH-1$^{fl/fl}$ and PINCH-1-K5 animals. All cells were immortalized by culturing primary cells long enough to let the spontaneous differentiation occur. ILK$^{fl/fl}$ and ILK-K5 cells were also isolated from the respective mouse line. The PINCH-1^{rescued} cell line was obtained by adenoviral infection of the PINCH-1–EGFP construct, followed by cell cloning. The colonies were tested for PINCH-1–EGFP expression and the colony with an endogenous expression level was chosen for further experiments (supplementary material Fig. S2D). All animal experiments were performed according to approved guidelines of the Max Planck Society and the government of Upper Bavaria.

Cell culture and transfection

Primary keratinocytes were isolated and cultured as described previously (Lorenz et al., 2007). To induce differentiation and the formation of cell–cell contacts keratinocytes were grown to confluence and treated with $CaCl_2$ at a final concentration of 1.2 mM. Transfections were carried out with Lipofectamine 2000 transfection reagent (Invitrogen). The following expression constructs were used: PINCH-1–EGFP (Braun et al., 2003; Stanchi et al., 2005), ILK–EGFP (Sakai et al., 2003), and EGFP or Cherry-tagged EPLIN, which were cloned by inserting the mouse EPLIN cDNA into the pEGFP-N1 (Clontech Laboratories Inc., Mountain View, CA) and pCherry-N1 (kindly obtained from Roger Y. Tsien, University California San Diego, La Jolla, CA) backbone, respectively.

Cell adhesion and spreading assays

Adhesion of epidermal keratinocytes to extracellular matrix proteins [Poly-L-lysine (Sigma), Col1 (Cohesion), fibronectin (Merck), LM332 (provided by Monique Aumailley, University of Cologne, Cologne, Germany)] was measured as previously described (Fässler et al., 1995).

For spreading assays, cells were seeded on ColI- and fibronectin-coated dishes and allowed to spread for the indicated times. Four images were taken every 15 min during the live-cell recording. All live-cell recordings were performed at 37℃ and under 5% CO_2 using a Zeiss Axiovert microscope equipped with a 10× NA0.3, 20× NA0.4, 40× NA0.6 and 100× NA1.3 objectives, a motorized scanning table (Märzhäuser) and a stage incubator (EMBL Precision Engineering, Heidelberg, Germany). Images were captured with a cooled CCD camera (Roper Scientific MicroMAX, Martinsried, Germany) using the Metamorph software (Molecular Devices, Sunnyvale, CA, USA) for microscope control and data acquisition.

TIRF microscopy

TIRF images were captured with an Axiovert 200M inverted microscope (Zeiss, Oberkochen, Germany) with a 100× oil objective and a CoolSnap HQ CCD camera (Photometrics, AZ). Acquisition was controlled by Metamorph Software (Molecular Devices, Sunnyvale, CA). Images were collected at 37℃.

Antibodies, immunohistochemistry and immunofluorescence staining

Immunohistochemistry of skin cryosections was carried out as described previously (Brakebusch et al., 2000). Immunostaining of cells were performed as described previously (Wickström et al., 2010b). The following antibodies and antibody dilutions were used: rat monoclonal antibody (mAb) against E-cadherin (1:400; Zymed); rabbit polyclonal antibody (pAb) against desmoplakin (1:500; Research Diagnostics, NV); rabbit pAb against EPLIN (1:150; Bethyl Laboratories, Inc.); mouse mAb against ILK (1:250; Millipore, MA); FITC-conjugated mAb against integrin α6 (1:400; BD Pharmingen, CA, USA), rat mAb against Ki67 (1:500; Dianova); rabbit pAb against LM332 (1:500; obtained from M. Aumailley); rat mAb against nidogen (1:500; Chemicon); rabbit pAb against Paxillin (1:50; Santa Cruz Biotechnology, USA); mouse mAb against PINCH (1:250; BD Biosciences); home-made rabbit pAb against PINCH-1 (Li et al., 2005); home-made rabbit pAb against PINCH-2; rabbit pAb against plakoglobin (1:500; Santa Cruz, USA); rat mAb against tubulin (1:300; clone YL 1/2, Millipore, MA, USA); mouse mAb against vinculin (1:300; Sigma-Aldrich, MO); phalloidin–Alexa-Fluor-488 (Life Technologies, NY); Phalloidin–TRITC (Sigma-Aldrich); goat anti mouse-IgG conjugated to Cy3; goat anti rat-IgG conjugated to Cy3; goat anti rabbit-IgG conjugated to Cy3; donkey anti-rabbit-IgG conjugated to Cy3 (Jackson Immunoresearch, PA, USA); goat anti-rabbit-IgG conjugated to Alexa Fluor 488 (Sigma-Aldrich, MO); goat anti-rat-IgG conjugated to Alexa Fluor 488 (Life Technologies, NY, USA); goat anti-rat-IgG conjugated to horseradish peroxidase (HRP), goat anti-mouse-IgG conjugated to HRP and goat anti-rabbit-IgG conjugated to HRP (BioRad, CA, USA). Fluorescence images were collected by confocal microscopy (DMIRE2; Leica, Wetzlar, Germany) using the Leica Confocal Software (version 2.5 Build 1227).

Proximity ligation assays

The PLA kit was purchased from Olink Bioscience (Uppsala, Sweeden). Every experiment was controlled with 'no antibody' and 'only one

antibody' conditions. As a representative control experiment, a 'no antibody' control is presented in Fig. 3E. Cells were cultured as described in the 'Cell culture and transfection' section. Cells were fixed with 4% PFA in PBS and stained according to the manufacturer's instructions.

Cell wounding assay

Cell wounding assays were performed with monolayers of keratinocytes treated with 4 µg/ml Mitomycin C (Sigma) for 4 h and then scratched with a 200 µl plastic micropipette to obtain wound widths of 500–600 µm. Wound closure was monitored with a Zeiss Axiovert microscope equipped with 10× NA0.3, 20× NA0.4, 40× NA0.6 and 100× NA1.3 objectives, a motorized scanning table (Märzhäuser) and a stage incubator (EMBL Precision Engineering, Heidelberg, Germany) for 12 h. Images were collected with a frame rate of one every 15 min using a cooled CCD camera (Roper Scientific MicroMAX, Martinsried, Germany) and Metamorph software (Molecular Devices, Sunnyvale, CA) was used for microscope control and data acquisition. All recordings were performed at 37℃ and under 5% CO_2.

Flow cytometry

Flow cytometry was carried out as previously described (Brakebusch et al., 2000). Antibodies used for FACS analysis were: FITC-conjugated hamster mAb against integrin β1; rat mAb against integrin β1 9EG7; FITC-conjugated rat mAb against integrin α6; biotinylated rat mAb against integrin αV; rat mAb against integrin β4; FITC-conjugated hamster mAb against integrin α2; biotinylated rat mAb against integrin α5 (all BD Biosciences, CA, USA); Streptavidin–Cy5 (BD Biosciences, CA, USA); mouse mAb anti-rat-IgG conjugated to FITC (BD Biosciences, CA, USA); goat anti mouse-FITC (Jackson Immunoresearch, PA, USA).

SDS-PAGE and immunoblotting

Cells were lysed in 50 mM Tris-HCl pH 8.0, 150 mM NaCl, 1% Triton X-100, 0.05% sodium deoxycholate and 10 mM EDTA supplemented with protease inhibitors (Roche, Penzberg, Germany) and phosphatase inhibitors (Sigma), homogenized in Laemmli buffer and boiled for 5 min. Cell lysates were electrophoretically separated on SDS-PAGE gels and then transferred onto nitrocellulose membranes, followed by incubation by antibodies. Bound antibodies were detected using enhanced chemiluminescence (Millipore Corporation, Billerica).

siRNA-mediated EPLIN depletion

siRNA duplexes for EPLIN and scrambled control duplexes were purchased from Sigma. Two siRNA duplexes (5′-GAAAUAGG-UGCGGGUCAUU-3′ and 5′-UGUAAGCCUCACUUCAAU-3′) were transfected with Lipofectamine (Life Technologies, NY, USA) into control or PINCH-1^{rescued} cells. Experiments were carried out 48 h after transfection.

Immunoprecipitation

Cell lysis and immunoprecipitation were performed as described previously (Böttcher et al., 2012). Briefly, cells were lysed with a buffer containing 150 mM NaCl, 50 mM Tris-HCl pH 7.5, 5% glycerol, 1% IGEPAL-CA-630, 1 mM $MgCl_2$ and protease inhibitors. Lysates were incubated with 50 µl magnetic beads coupled with monoclonal mouse anti-GFP antibody (Miltenyi Biotec GmbH, Bergisch Gladbach, Germany). After washes, proteins were pre-digested on the same column with trypsin, eluted from the column with DTT and further digested with trypsin overnight. Peptides were purified on C_{18} StageTips before mass spectrometry analysis.

LC-MS/MS analysis

Peptides were separated by reverse-phase chromatography coupled to liquid chromatography tandem mass spectrometry (LC-MS/MS) analysis using an LTQ-Orbitrap Velos mass spectrometer (Thermo Fisher Scientific, MA). Peptide separation was performed with an EASY-nanoLC system (Thermo Fisher Scientific, MA) with a 180-min gradient from 5% to 35% buffer B (80% acetonitrile, 0.5% acetic acid). In the mass spectrometry method, full scans were acquired in the Orbitrap with a resolution of 60,000. The top ten most intense ions were fragmented by collision-induced dissociation (CID), and MS/MS spectra were acquired in the LTQ.

The raw files from the mass spectrometry were processed with the MaxQuant software version 1.0.13.13 (Cox and Mann, 2008). Data were searched against the forward and decoy database (pi.MOUSE.v3.62.decoy.fasta) using the Mascot search engine. Fixed modifications were carbamidomethylated cysteins and variable modifications were oxidation of methionine, and N-terminal acetylation. Maximum false discovery rates (FDR) were set to 0.01 both on peptide and protein levels. Proteins were quantified using the label-free algorithm in MaxQuant. To extract significant binders we performed a two-sample Student's *t*-test between triplicates, with 0.1 FDR.

Statistics

Results are shown as mean±s.d. where indicated. Significance was determined by unpaired Student's *t*-test and where necessary a Mann–Whitney U test was also applied.

Competing interests

The authors declare no competing or financial interests.

Author contributions

R.F. designed, conceptualized the study and wrote the manuscript. E.K., K.F., K.L.B. acquired and analyzed data. T.G. and M.M. acquired, analyzed and interpreted mass spectrometry data. R.Z. helped in designing experiments and critically revised the manuscript.

Funding

This work was funded by the National Institutes of Health [grant numbers RO1-DK083187, RO1-DK075594, R01-DK069221 to R.Z.]; and a VA Merit Award [grant number 1I01BX002196 to R.Z.]; and by the European Research Council (ERC) (to R.F.); and the Max Planck Society (to R.F.). Deposited in PMC for release after 12 months.

Supplementary material

Supplementary material available online at
http://jcs.biologists.org/lookup/suppl/doi:10.1242/jcs.162545/-/DC1

References

Abe, K. and Takeichi, M. (2008). EPLIN mediates linkage of the cadherin catenin complex to F-actin and stabilizes the circumferential actin belt. *Proc. Natl. Acad. Sci. USA* **105**, 13-19.

Azimifar, S. B., Böttcher, R. T., Zanivan, S., Grashoff, C., Krüger, M., Legate, K. R., Mann, M. and Fässler, R. (2012). Induction of membrane circular dorsal ruffles requires co-signalling of integrin-ILK-complex and EGF receptor. *J. Cell Sci.* **125**, 435-448.

Baum, B. and Georgiou, M. (2011). Dynamics of adherens junctions in epithelial establishment, maintenance, and remodeling. *J. Cell Biol.* **192**, 907-917.

Bock-Marquette, I., Saxena, A., White, M. D., Dimaio, J. M. and Srivastava, D. (2004). Thymosin beta4 activates integrin-linked kinase and promotes cardiac cell migration, survival and cardiac repair. *Nature* **432**, 466-472.

Bokoch, G. M., Wang, Y., Bohl, B. P., Sells, M. A., Quilliam, L. A. and Knaus, U. G. (1996). Interaction of the Nck adapter protein with p21-activated kinase (PAK1). *J. Biol. Chem.* **271**, 25746-25749.

Böttcher, R. T., Stremmel, C., Meves, A., Meyer, H., Widmaier, M., Tseng, H. Y. and Fässler, R. (2012). Sorting nexin 17 prevents lysosomal degradation of β1 integrins by binding to the β1-integrin tail. *Nat. Cell Biol.* **14**, 584-592.

Brakebusch, C., Grose, R., Quondamatteo, F., Ramirez, A., Jorcano, J. L., Pirro, A., Svensson, M., Herken, R., Sasaki, T., Timpl, R. et al. (2000). Skin and hair follicle integrity is crucially dependent on beta 1 integrin expression on keratinocytes. *EMBO J.* **19**, 3990-4003.

Braun, A., Bordoy, R., Stanchi, F., Moser, M., Kostka G, G., Ehler, E., Brandau, O. and Fässler, R. (2003). PINCH2 is a new five LIM domain protein, homologous to PINCHand localized to focal adhesions. *Exp. Cell Res.* **284**, 237-248.

Braverman, L. E. and Quilliam, L. A. (1999). Identification of Grb4/Nckbeta, a src homology 2 and 3 domain-containing adapter protein having similar binding and biological properties to Nck. *J. Biol. Chem.* **274**, 5542-5549.

Chiswell, B. P., Zhang, R., Murphy, J. W., Boggon, T. J. and Calderwood, D. A. (2008). The structural basis of integrin-linked kinase-PINCH interactions. *Proc. Natl. Acad. Sci. USA* **105**, 20677-20682.

Chiswell, B. P., Stiegler, A. L., Razinia, Z., Nalibotski, E., Boggon, T. J. and Calderwood, D. A. (2010). Structural basis of competition between PINCH1 and PINCH2 for binding to the ankyrin repeat domain of integrin-linked kinase. *J. Struct. Biol.* **170**, 157-163.

Cox, J. and Mann, M. (2008). MaxQuant enables high peptide identification rates, individualized p.p.b.-range mass accuracies and proteome-wide protein quantification. *Nat. Biotechnol.* **26**, 1367-1372.
Dowling, J., Yu, Q. C. and Fuchs, E. (1996). Beta4 integrin is required for hemidesmosome formation, cell adhesion and cell survival. *J. Cell Biol.* **134**, 559-572.
Fässler, R., Pfaff, M., Murphy, J., Noegel, A. A., Johansson, S., Timpl, R. and Albrecht, R. (1995). Lack of beta 1 integrin gene in embryonic stem cells affects morphology, adhesion, and migration but not integration into the inner cell mass of blastocysts. *J. Cell Biol.* **128**, 979-988.
Fielding, A. B., Dobreva, I. and Dedhar, S. (2008a). Beyond focal adhesions: integrin-linked kinase associates with tubulin and regulates mitotic spindle organization. *Cell Cycle* **7**, 1899-1906.
Fielding, A. B., Dobreva, I., McDonald, P. C., Foster, L. J. and Dedhar, S. (2008b). Integrin-linked kinase localizes to the centrosome and regulates mitotic spindle organization. *J. Cell Biol.* **180**, 681-689.
Gates, J. and Peifer, M. (2005). Can 1000 reviews be wrong? Actin, alpha-Catenin, and adherens junctions. *Cell* **123**, 769-772.
Grose, R., Hutter, C., Bloch, W., Thorey, I., Watt, F. M., Fässler, R., Brakebusch, C. and Werner, S. (2002). A crucial role of beta 1 integrins for keratinocyte migration in vitro and during cutaneous wound repair. *Development* **129**, 2303-2315.
Han, M. Y., Kosako, H., Watanabe, T. and Hattori, S. (2007). Extracellular signal-regulated kinase/mitogen-activated protein kinase regulates actin organization and cell motility by phosphorylating the actin cross-linking protein EPLIN. *Mol. Cell. Biol.* **27**, 8190-8204.
Jamora, C. and Fuchs, E. (2002). Intercellular adhesion, signalling and the cytoskeleton. *Nat. Cell Biol.* **4**, E101-E108.
Legate, K. R., Montañez, E., Kudlacek, O. and Fässler, R. (2006). ILK, PINCH and parvin: the tIPP of integrin signalling. *Nat. Rev. Mol. Cell Biol.* **7**, 20-31.
Lenter, M., Uhlig, H., Hamann, A., Jenö, P. and Vestweber, D. (1993). A monoclonal antibody against an activation epitope on mouse integrin β 1 blocks adhesion of lymphocytes to the endothelial integrin α 6 β 1. *Pro. Natl. Acad. Sci. USA* **90**, 9051-9055.
Li, S., Bordoy, R., Stanchi, F., Moser, M., Braun, A., Kudlacek, O., Wewer, U. M., Yurchenco, P. D. and Fässler, R. (2005). PINCH1 regulates cell-matrix and cell-cell adhesions, cell polarity and cell survival during the peri-implantation stage. *J. Cell Sci.* **118**, 2913-2921.
Liang, X., Zhou, Q., Li, X., Sun, Y., Lu, M., Dalton, N., Ross, J., Jr and Chen, J. (2005). PINCH1 plays an essential role in early murine embryonic development but is dispensable in ventricular cardiomyocytes. *Mol. Cell. Biol.* **25**, 3056-3062.
Lorenz, K., Grashoff, C., Torka, R., Sakai, T., Langbein, L., Bloch, W., Aumailley, M. and Fässler, R. (2007). Integrin-linked kinase is required for epidermal and hair follicle morphogenesis. *J. Cell Biol.* **177**, 501-513.
Margadant, C., Raymond, K., Kreft, M., Sachs, N., Janssen, H. and Sonnenberg, A. (2009). Integrin alpha3beta1 inhibits directional migration and wound re-epithelialization in the skin. *J. Cell Sci.* **122**, 278-288.
Maul, R. S. and Chang, D. D. (1999). EPLIN, epithelial protein lost in neoplasm. *Oncogene* **18**, 7838-7841.
Maul, R. S., Song, Y., Amann, K. J., Gerbin, S. C., Pollard, T. D. and Chang, D. D. (2003). EPLIN regulates actin dynamics by cross-linking and stabilizing filaments. *J. Cell Biol.* **160**, 399-407.
Mège, R. M., Gavard, J. and Lambert, M. (2006). Regulation of cell-cell junctions by the cytoskeleton. *Curr. Opin. Cell Biol.* **18**, 541-548.
Nakrieko, K. A., Welch, I., Dupuis, H., Bryce, D., Pajak, A., St Arnaud, R., Dedhar, S., D'Souza, S. J. and Dagnino, L. (2008). Impaired hair follicle morphogenesis and polarized keratinocyte movement upon conditional inactivation of integrin-linked kinase in the epidermis. *Mol. Biol. Cell* **19**, 1462-1473.
Niculescu, C., Ganguli-Indra, G., Pfister, V., Dupé, V., Messaddeq, N., De Arcangelis, A. and Georges-Labouesse, E. (2011). Conditional ablation of integrin alpha-6 in mouse epidermis leads to skin fragility and inflammation. *Eur. J. Cell Biol.* **90**, 270-277.
Raghavan, S., Bauer, C., Mundschau, G., Li, Q. and Fuchs, E. (2000). Conditional ablation of beta1 integrin in skin. Severe defects in epidermal proliferation, basement membrane formation, and hair follicle invagination. *J. Cell Biol.* **150**, 1149-1160.
Ramirez, A., Page, A., Gandarillas, A., Zanet, J., Pibre, S., Vidal, M., Tusell, L., Genesca, A., Whitaker, D. A., Melton, D. W. et al. (2004). A keratin K5Cre transgenic line appropriate for tissue-specific or generalized Cre-mediated recombination. *Genesis* **39**, 52-57.
Rodius, S., Indra, G., Thibault, C., Pfister, V. and Georges-Labouesse, E. (2007). Loss of alpha6 integrins in keratinocytes leads to an increase in TGFbeta and AP1 signaling and in expression of differentiation genes. *J. Cell. Physiol.* **212**, 439-449.
Sakai, T., Li, S., Docheva, D., Grashoff, C., Sakai, K., Kostka, G., Braun, A., Pfeifer, A., Yurchenco, P. D. and Fässler, R. (2003). Integrin-linked kinase (ILK) is required for polarizing the epiblast, cell adhesion, and controlling actin accumulation. *Genes Dev.* **17**, 926-940.
Schaller, V., Schmoller, K. M., Karakose, E., Hammerich, B., Maiera, M. and Bausch, A. R. (2013). Crosslinking proteins modulate the self-organization of driven systems. *Soft Matter* **9**, 7229-7233.
Schiller, H. B., Friedel, C. C., Boulegue, C. and Fässler, R. (2011). Quantitative proteomics of the integrin adhesome show a myosin II-dependent recruitment of LIM domain proteins. *EMBO Rep.* **12**, 259-266.
Schlöndorff, D. and Banas, B. (2009). The mesangial cell revisited: no cell is an island. *J. Am. Soc. Nephrol.* **20**, 1179-1187.
Sehgal, B. U., DeBiase, P. J., Matzno, S., Chew, T. L., Claiborne, J. N., Hopkinson, S. B., Russell, A., Marinkovich, M. P. and Jones, J. C. (2006). Integrin beta4 regulates migratory behavior of keratinocytes by determining laminin-332 organization. *J. Biol. Chem.* **281**, 35487-35498.
Stanchi, F., Bordoy, R., Kudlacek, O., Braun, A., Pfeifer, A., Moser, M. and Fässler, R. (2005). Consequences of loss of PINCH2 expression in mice. *J. Cell Sci.* **118**, 5899-5910.
Taguchi, K., Ishiuchi, T. and Takeichi, M. (2011). Mechanosensitive EPLIN-dependent remodeling of adherens junctions regulates epithelial reshaping. *J. Cell Biol.* **194**, 643-656.
Tsurumi, H., Harita, Y., Kurihara, H., Kosako, H., Hayashi, K., Matsunaga, A., Kajiho, Y., Kanda, S., Miura, K., Sekine, T. et al. (2014). Epithelial protein lost in neoplasm modulates platelet-derived growth factor-mediated adhesion and motility of mesangial cells. *Kidney Int.* **86**, 548-557.
Tu, Y., Li, F. and Wu, C. (1998). Nck-2, a novel Src homology2/3-containing adaptor protein that interacts with the LIM-only protein PINCH and components of growth factor receptor kinase-signaling pathways. *Mol. Biol. Cell* **9**, 3367-3382.
Tu, Y., Kucik, D. F. and Wu, C. (2001). Identification and kinetic analysis of the interaction between Nck-2 and DOCK180. *FEBS Lett.* **491**, 193-199.
van der Neut, R., Krimpenfort, P., Calafat, J., Niessen, C. M. and Sonnenberg, A. (1996). Epithelial detachment due to absence of hemidesmosomes in integrin beta 4 null mice. *Nat. Genet.* **13**, 366-369.
Watt, F. M. (2002). Role of integrins in regulating epidermal adhesion, growth and differentiation. *EMBO J.* **21**, 3919-3926.
Wickström, S. A., Lange, A., Montanez, E. and Fässler, R. (2010a). The ILK/PINCH/parvin complex: the kinase is dead, long live the pseudokinase! *EMBO J.* **29**, 281-291.
Wickström, S. A., Lange, A., Hess, M. W., Polleux, J., Spatz, J. P., Krüger, M., Pfaller, K., Lambacher, A., Bloch, W., Mann, M. et al. (2010b). Integrin-linked kinase controls microtubule dynamics required for plasma membrane targeting of caveolae. *Dev. Cell* **19**, 574-588.
Zhang, Y., Chen, K., Tu, Y., Velyvis, A., Yang, Y., Qin, J. and Wu, C. (2002). Assembly of the PINCH-ILK-CH-ILKBP complex precedes and is essential for localization of each component to cell-matrix adhesion sites. *J. Cell Sci.* **115**, 4777-4786.

SUPPLEMENTARY FIGURES

Supplementary Figure 1: PINCH protein levels and skin histology of P1-K5 mice

(**A**) PINCH and ILK protein levels in epidermal lysates of control and P1-K5 mice at P0, P7, P14 and P56. GAPDH served as loading control. **(B**) Western blot analyses of PINCH-1 and PINCH-2 in bacterial lysates that express pGEX-PINCH-1, pGEX-PINCH-2, in fibroblasts and in epidermal lysates from control and P1-K5 skin at P14. Note that highly specific home-made PINCH-1 and PINCH-2 antibodies are used. (**C**) Western blot analyses of PINCH-2 and PINCH in epidermal lysates of control and P1-K5 mice at P0, P7, P14 and P56. PINCH-2 levels were tested by home-made PINCH-2 antibody and PINCH levels were determined by pan-PINCH antibody. GAPDH served as loading control. (**D**) Immunostaining of Nidogen and PINCH on sections from P0 back skin. (**E**) Quantification of blisters per mm in control and P1-K5 epidermis. Back skin sections from 3 different mice were used for each genotype. Bars represent standard deviation. (**F**) Ki67 staining on P7 back skin. Note the presence of suprabasal proliferating cells in P1-K5 epidermis. (**G**) High magnification of hematoxylin-eosin stained HFs from P14 back skin. (**H**) Nidogen staining on P14 back skin. Arrowheads mark the BM (control) and suprabasal localization of nidogen (P1-K5). ORS: Outer root sheet; DP: Dermal papilla; Epidermis (e); Dermis (d). Bars represent 50 μm (D, F, G, H).

Supplementary Figure 2: Integrin expression analysis and altered F-actin distribution in PINCH knockout keratinocytes

(**A**) Cell surface expression of integrins on freshly isolated keratinocytes determined by FACS (black histogram: control cells; red: P1-K5 cells; dashed histograms: negative controls). The antibody β1 Ha2/5 recognizes total β1 integrin and 9EG7 reports a ligand-induced binding site and hence the active β1 integrin. (**B**) F-actin staining of keratinocytes grown on a FN/Col1 matrix after differentiation with $CaCl_2$. Panels show top and bottom of each stack. Note that the actin distribution is severely altered at the bottom side of PINCH-1 -/- cells. **(C**) Schematic illustration of the workflow to obtain PINCH-1 interactors. (**D**) Western blot analysis of protein lysates from PINCH-1 fl/fl, PINCH-1 -/- and $PINCH1^{rescued}$ keratinocytes. GAPDH served as loading control. (**E**) Spreading quantification of PINCH-1 fl/fl, PINCH-1 -/- and $PINCH1^{rescued}$ cells. (**F**) Immunostaining of immortalized and cloned PINCH-1 fl/fl, PINCH-1 -/- and $PINCH1^{rescued}$ keratinocytes. Bars represent 50 μm (B, F).

Supplementary Figure 3: Characterization of the novel PINCH-1-interacting protein, EPLIN

(**A**) Immunostainings of relevant PLA controls. Note that the red dots are only obviously visible in the most right panel. (**B**) Immunostaining of Nidogen (red) and EPLIN (green) in P14 control and P1-K5 back skin sections. DAPI (blue) shows nuclei. In control sections (left panel), EPLIN staining is homogeneous in epithelial cells with roughly equal staining at the basal surface (white arrowheads) and in the cytoplasm or near cell-cell contacts (open arrowheads). In P1-K5 skin sections (right panels), EPLIN localization is more irregular with intermittant regions of low EPLIN levels on the basal surfaces (white arrowheads) relative to the high levels in the cytoplasm (open arrowheads). While Nidogen staining clearly indicates the well-defined basement membrane in control skin sections (red arrowhead), it is deposited abnormally in the epidermis of P1-K5 skin (red arrowheads). (**C**) Immunostaining of EPLIN-depleted and $CaCl_2$-treated immortalized keratinocytes for EPLIN and E-cadherin. Bars represent 50 μm.

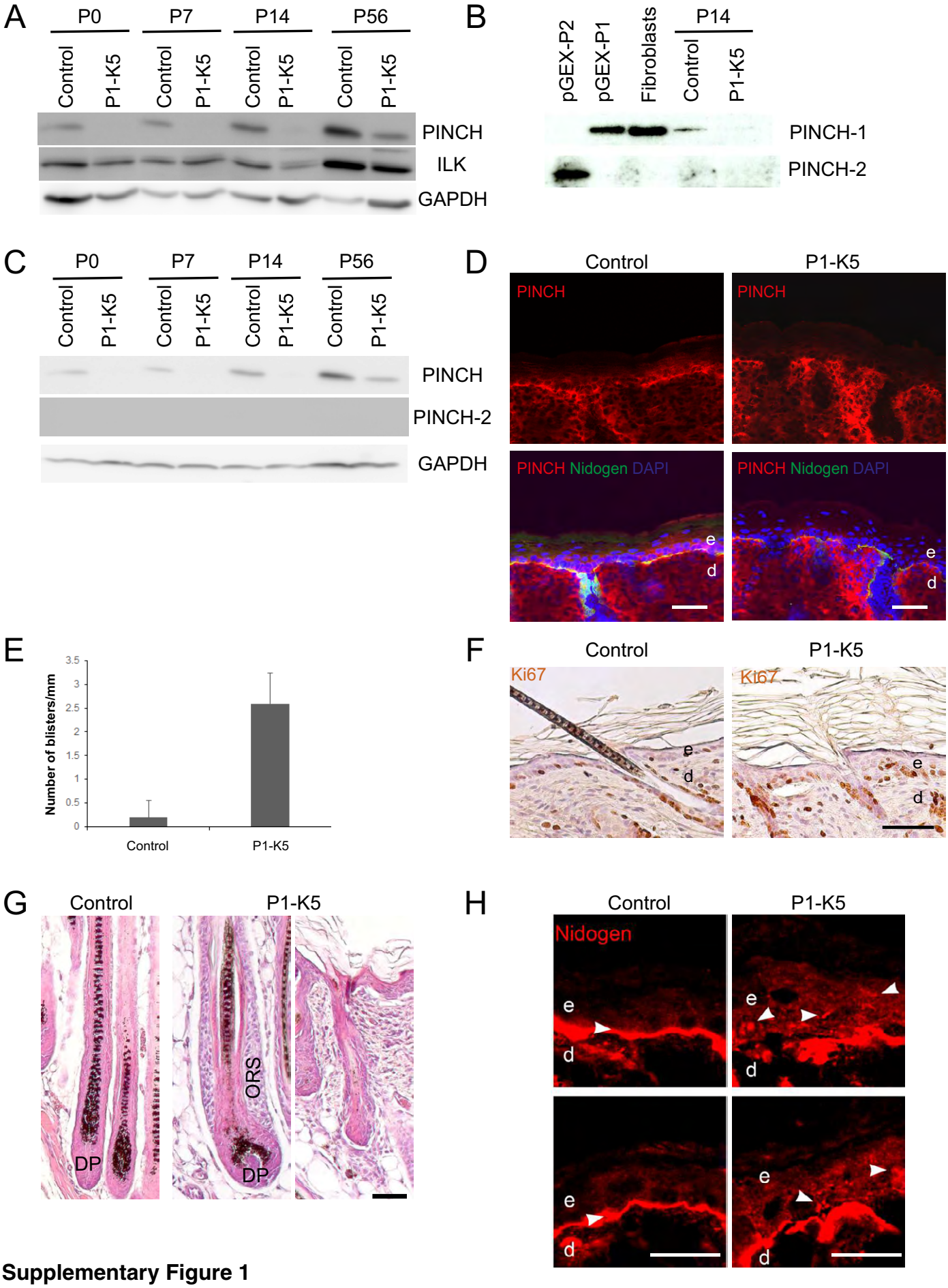

Supplementary Figure 1

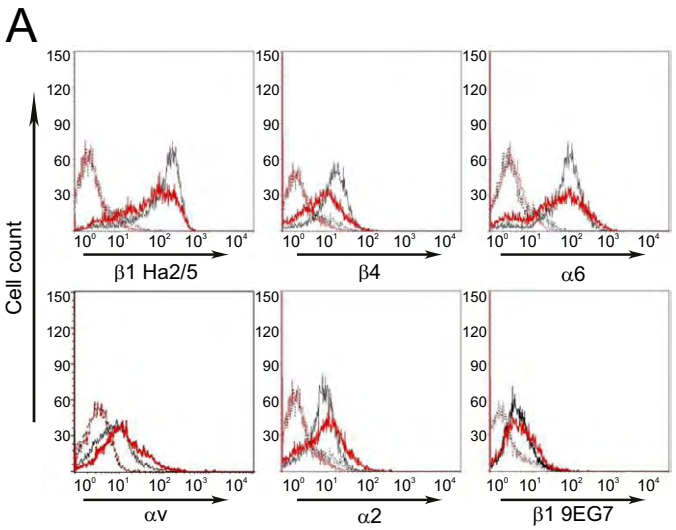

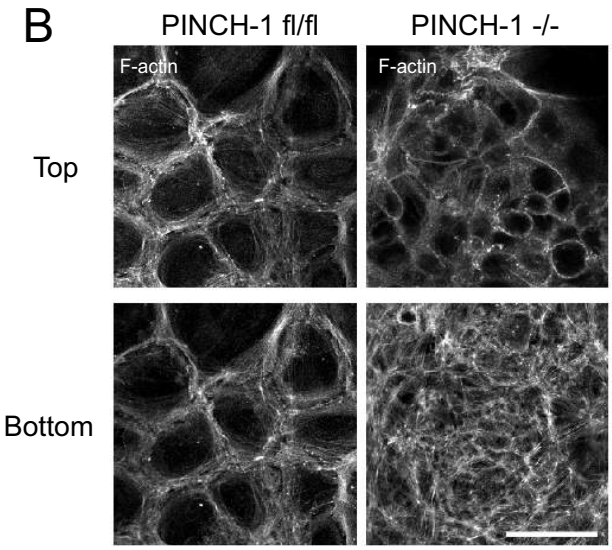

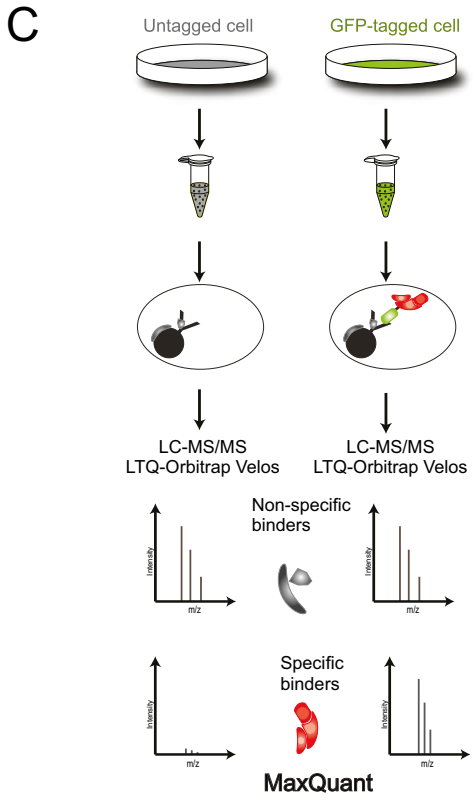

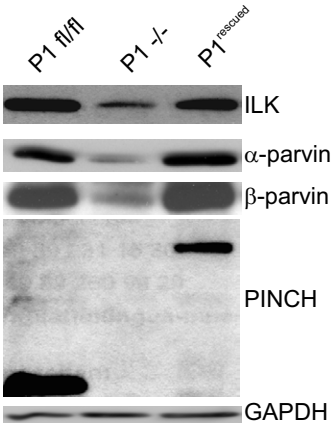

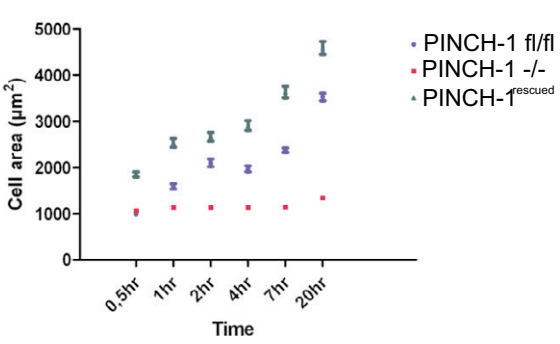

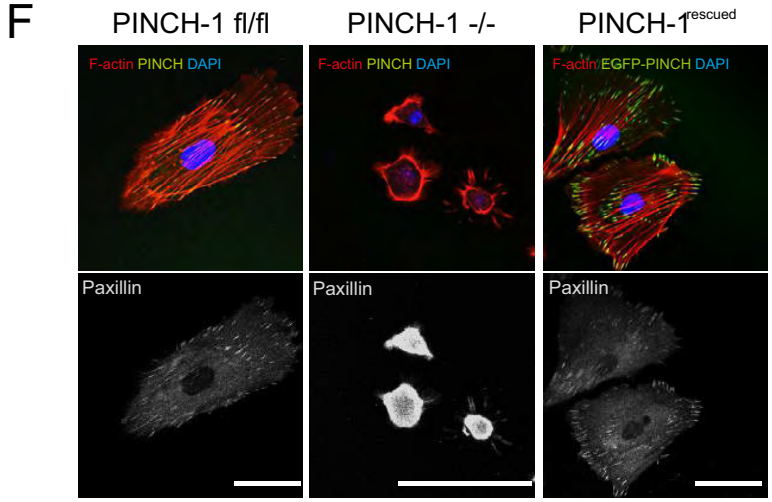

Supplementary Figure 2

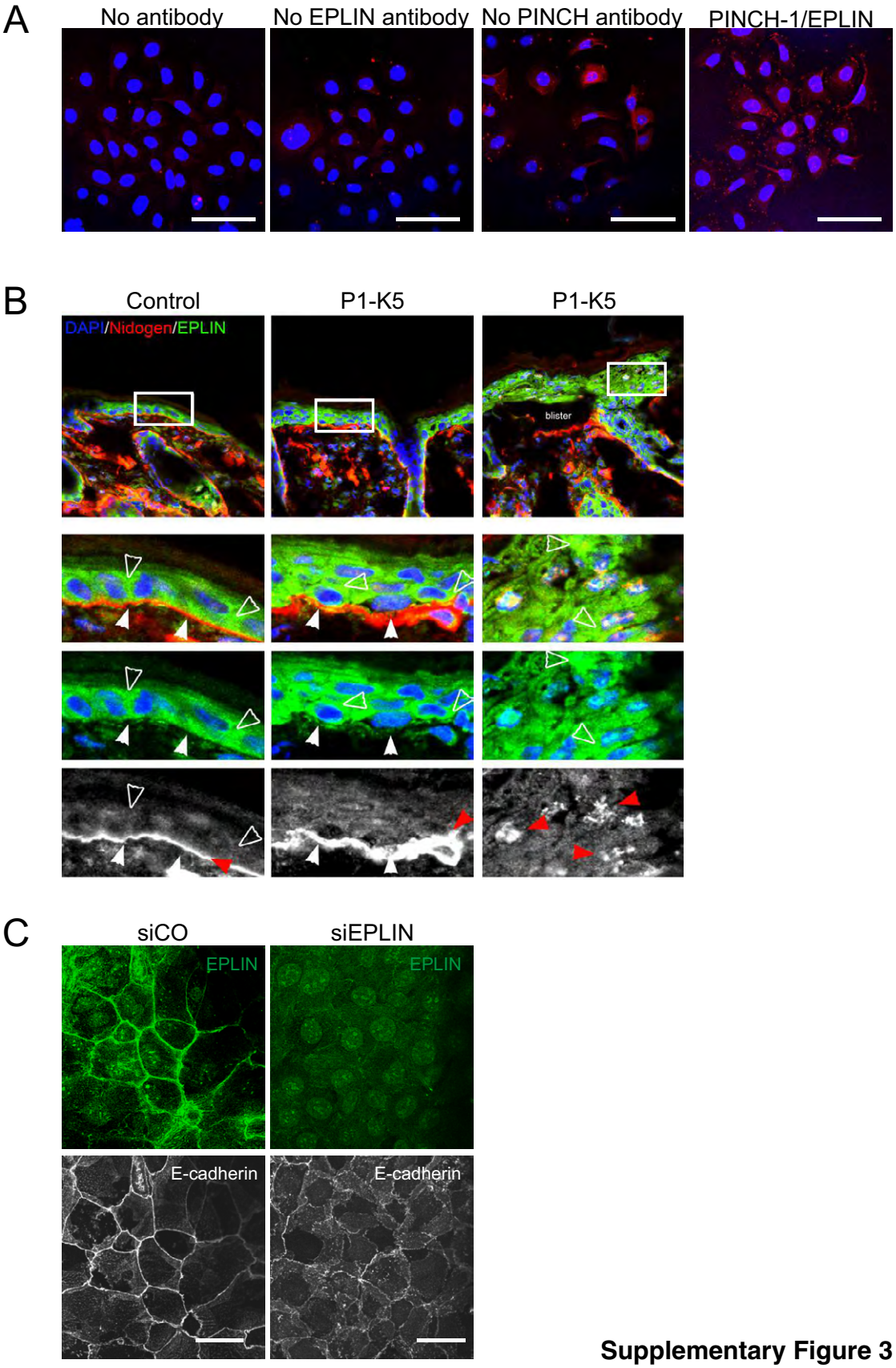

Supplementary Figure 3

Table S1.

Download Table S1